ACS APPLIED MATERIALS & INTERFACES

Research Article

www.acsami.org

# Dithiophenedione-Containing Polymers for Battery Application

Bernhard Häupler,[†,‡] Tino Hagemann,[†,‡] Christian Friebe,[†,‡] Andreas Wild,[†,‡] and Ulrich S. Schubert*[,†,‡]

[†]Laboratory of Organic and Macromolecular Chemistry, Friedrich Schiller University Jena, Humboldtstraße 10, 07743 Jena, Germany

[‡]Center for Energy and Environmental Chemistry (CEEC Jena), Friedrich Schiller University Jena, Philosophenweg 7a, 07743 Jena, Germany

Supporting Information

**ABSTRACT:** Redox-active polymers have received recently significant interest as active materials in secondary organic batteries. We designed a redox-active monomer, namely 2-vinyl-4,8-dihydrobenzo[1,2-b:4,5-b′]-dithiophene-4,8-dione that exhibits two one-electron redox reactions and has a low molar mass, resulting in a high theoretical capacity of 217 mAh/g. The free radical polymerization of the monomer was optimized by variation of solvent and initiator. The electrochemical behavior of the obtained polymer was investigated using cyclic voltammetry. The utilization of lithium salts in the supporting electrolyte leads to a merging of the redox waves accompanied by a shift to higher redox potentials. Prototype batteries manufactured with 10 wt % polymer as active material exhibit full material activity at the first charge/discharge cycle. During the first 100 cycles, the capacity drops to 50%. Higher contents of polymer (up to 40 wt %) leads to a lower material activity. Furthermore, the battery system reveals a fast charge/discharge ability, allowing a maximum speed up to 10C (6 min) with only a negligible loss of capacity.

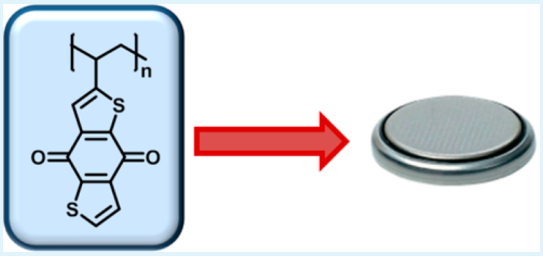


**KEYWORDS:** *redox-active, polymer, quinone, cathode material, organic battery*

## 1. INTRODUCTION

Electrodes in commercially available secondary batteries are in general made of inorganic materials, i.e., mainly metals. The majority of these metals are heavy, expensive and some are toxic. In contrast, batteries based on organic molecules contain elements such as carbon, hydrogen, nitrogen, oxygen and/or sulfur, allowing a residue-free disposal and the generation from renewable resources.[1] Other beneficial properties are low toxicity, flexibility, and lightweight,[2] as well as the possibility to tune the cell potential through the design of the redox-active molecules. A large variety of organic redox-active compounds was applied as active electrode materials in batteries, such as stable organic radicals[3,4] and organic sulfur compounds.[5] Of particular interest are also quinonide structures, because of their two-electron redox behavior, accompanied by a low molar mass, resulting in a high theoretical capacity. Therefore, a number of different quinonide structures were already applied as active electrode materials in secondary batteries. The very first attempts were accomplished by Alt et al., who studied the reversible solid-state reduction of chloranil in organic and aqueous electrolytes.[6,7] Several other quinonide-based small molecules such as benzoquinone,[8,9] phenanthrenequinone,[10] and anthraquinone,[11] and their derivates[12−15] were studied, but their charge/discharge stability is often poor, caused by dissolution of the small molecules in the electrolyte. Different approaches to improve the stability of small quinonide molecules have been undertaken: The introduction of functional groups that diminish the solubility[1] like sulfonic acids,[16,17] carboxylic acids,[18] and their lithium and sodium salts, the utilization of quasi-solid-state electrolytes,[19] or the incorporation of the redox-active unit into a polymer in the backbone or side chain. Thereby, first approaches used polymers with quinone units in the backbone. Several examples revealed a high capacity accompanied by a good cycling stability.[20−25] These polymers were mainly synthesized by polycondensation or polyaddition reactions and are, therefore, often insoluble, nonswellable, and/or tend to crystallize. Redox-active polymers with pendant quinonide structures are difficult to synthesize, due to radical and ion-trapping properties. Two polymers were synthesized by polymer-analogous reactions and were successfully applied as active battery material. Both the condensation of poly(4-chloromethylstyrene) with anthraquinone-2-carboxylic acid[26] and the reaction of poly(methacryloyl chloride) with pyrene-4,5,9,10-tetraone[27] led to polymers with excellent charge/discharge properties. The drawback of the polymer-analogous reaction is the incomplete functionalization. Although quinones are known as radical scavengers, Nishide and co-workers were able to polymerize 2-vinylanthraquinone using free radical polymerization techniques.[28] This polymer displays an excellent performance as active material in a secondary organic air battery with aqueous electrolyte.

In this study, we report the synthesis of poly(2-vinyl-4,8-dihydrobenzo[1,2-b:4,5-b′]dithiophene-4,8-dione) (PVBDT). The polymer was applied as active cathode material in

Received: September 7, 2014
Accepted: January 22, 2015
Published: January 22, 2015





DOI: 10.1021/am5060959
ACS Appl. Mater. Interfaces 2015, 7, 3473−3479

Table 1. Overview of Selected Properties of the Polymers Obtained by Free Radical Polymerizations Using Different Solvent/Initiator Systems

| solvent | conc. [mol/L] | initiator | $c_{ini}$ [mol %] | temp. (°C) | yield (%) | $M_n$ [g/mol] | $M_w$ [g/mol] |
|---|---|---|---|---|---|---|---|
| DCE | 0.25 | AIBN | 5 | 70 | 8 | $2.49 \times 10^3$ | $8.03 \times 10^3$ |
| DMSO | 0.5 | AIBN | 5 | 70 | 25 | $4.72 \times 10^3$ | $1.99 \times 10^4$ |
| DMF | 0.5 | AIBN | 5 | 70 | 15 | $4.11 \times 10^3$ | $1.64 \times 10^4$ |
| DMAc | 0.5 | AIBN | 5 | 70 | 25 | $2.72 \times 10^3$ | $1.01 \times 10^4$ |
| NMP | 1 | AIBN | 5 | 70 | 40 | $2.62 \times 10^3$ | $9.28 \times 10^4$ |
| NMP | 1 | *t*-BuOOH | 5 | 130 | 48 | $2.63 \times 10^3$ | $1.96 \times 10^4$ |
| NMP | 1 | ACHN | 5 | 100 | 45 | $3.77 \times 10^3$ | $1.98 \times 10^4$ |
| NMP | 1 | Luperox 101 | 5 | 100 | 33 | $3.85 \times 10^3$ | $8.85 \times 10^3$ |
| NMP | 1 | *t*-BuOOCOPh | 5 | 100 | 56 | $3.18 \times 10^3$ | $2.21 \times 10^4$ |
| NMP | 1 | *t*-BuOO*t*-Bu | 5 | 130 | 40 | $2.29 \times 10^3$ | $1.62 \times 10^4$ |
| NMP | 1 | *t*-BuOOCOPh | 10 | 100 | 49 | $3.26 \times 10^3$ | $4.22 \times 10^4$ |
| NMP | 1 | *t*-BuOOCOPh | 1 | 100 | 57 | $2.98 \times 10^3$ | $3.31 \times 10^4$ |

lithium-organic batteries and the charge/discharge properties of the polymer in a composite electrode at different charging speeds and different ratios of active material to conductive additive were investigated.

## 2. EXPERIMENTAL SECTION

**2.1. Methods.** Dichloromethane and toluene were dried with a PureSolv-EN Solvent Purification System (Innovative Technology). *N*,*N*′-Dimethylformamide (DMF) was distilled over calcium hydride and stored over molecular sieves. 1,2-Dichloroethane (DCE) was distilled over $P_2O_5$ and stored over molecular sieves. *N*,*N*′-Dimethylacetamide (DMAc), *N*-methyl-2-pyrrolidone (NMP), and dimethyl sulfoxide (DMSO) were purchased from Sigma-Aldrich in anhydrous quality. 2,2′-Azo*bis*(*iso*-butyronitrile) (AIBN) was recrystallized from methanol prior to use. 4,8-Dihydrobenzo[1,2-b:4,5-b′]dithiophene-4,8-dione (**1**) was synthesized according to a literature procedure.[29] All other starting materials were purchased from commercial sources and were used as obtained. Reactions were monitored by TLC on 0.2 mm Merck silica gel plates (60 F254). Column chromatography was performed on silica gel 60 (Merck). $^1$H and $^{13}$C NMR spectra were recorded on a Bruker AC 300 (300 MHz) spectrometer at 298 K. Chemical shifts are reported in parts per million (ppm, $\delta$ scale) relative to the residual signal of the deuterated solvent. Elemental analyses were carried out using a Vario ELIII—Elementar Euro and an EA—HekaTech. Cyclic voltammetry and galvanostatic experiments were performed using a Biologic VMP 3 potentiostat at room temperature under argon atmosphere. Size-exclusion chromatography was performed on an Agilent 1200 series system (degasser, PSS; pump, G1310A; auto sampler, G1329A; oven, Techlab; DAD detector, G1315D; RI detector, G1362A; eluent, DMAc + 0.21% LiCl, 1 mL/min; temperature, 40 °C; column, PSS GRAM guard/1000/30 Å). Spectroelectrochemical experiments were carried out in a quartz cuvette containing the respective electrolyte solution, a platinum grid working electrode, a platinum wire auxiliary electrode, and a $AgNO_3$/Ag reference electrode. The potential was controlled using a Metrohm Autolab PGSTAT30 potentiostat. The oxidation process was monitored by UV—vis spectroscopy using a PerkinElmer Lambda 750 UV-vis spectrophotometer and considered complete when there was no further spectral change.

**2.2. Synthesis of 2-Iodobenzo[1,2-b:4,5-b′]dithiophene-4,8-dione (2).** 4,8-Dihydrobenzo[1,2-b:4,5-b′]dithiophene-4,8-dione (**1**) (3.72 g, 16.88 mmol), silver sulfate (5.79 g, 18.57 mmol, 1.1 equiv), silver trifluoromethanesulfonate (0.65 g, 2.53 mmol, 0.15 equiv), and iodine (4.71 g, 18.57 mmol, 1.1 equiv) were dissolved in 169 mL of dichloromethane under argon atmosphere and stirred at room temperature for 18 h. The precipitate was separated by filtration, and the reaction mixture was washed successively with saturated sodium sulfite solution (150 mL), water (150 mL), brine (100 mL), dried over sodium sulfate, filtered, and concentrated under reduced pressure. The residue was purified by column chromatography ($SiO_2$ 60, $CHCl_3$) to yield 4.85 g (83%) of 2-iodobenzo[1,2-b:4,5-b′]dithiophene-4,8-dione (**2**) as a red powder. EI-MS (*m*/*z*): 346, 318, 219, 191, 163, 119, 95, 81, 45. $^1$H NMR ($CD_2Cl_2$, 300 MHz, ppm): $\delta$ 7.82 (s, 1H), 7.78 (d, 1H), 7.63 (d, 1H). $^{13}$C NMR ($CD_2Cl_2$ 75 MHz, ppm): 173.02, 142.36, 135.96, 134.09, 126.34, 85,51. Anal. Calcd for $C_{10}H_3IO_2S_2$: C, 34.70; H, 0.87; O, 9.24. Found: C, 34.80; H, 0.97; O, 9.31.

**2.3. Synthesis of 2-Vinylbenzo[1,2-b:4,5-b′]dithiophene-4,8-dione (3).** 2-Iodobenzo[1,2-b:4,5-b′]dithiophene-4,8-dione (937 mg, 2.71 mmol), 2,6-di-*tert*-butylhydroxytoluene (11.93 mg, 0.054 mmol, 0.02 equiv), and tetrakis(triphenylphosphine)palladium(0) (165 mg, 0.135 mmol, 0.05 equiv) were dissolved in 18 mL of DMF under argon atmosphere. Tributylstannylethylene (1.19 mL, 4.06 mmol, 1.5 equiv) was added dropwise via a syringe, and the reaction mixture was stirred under reflux at 100 °C for 16 h. Toluene was evaporated under reduced pressure, and the residue was purified by column chromatography ($SiO_2$ 60, $CHCl_3$:*n*-hexane 4:1) to yield 581 mg (87%) of 2-vinylbenzo[1,2-b:4,5-b′]dithiophene-4,8-dione (**3**) as an orange solid. EI-MS (*m*/*z*): 246, 218, 190, 145, 109, 82, 71, 45. $^1$H NMR ($CDCl_3$, 300 MHz, ppm): 7.71 (d, 1H), 7.66 (d, 1H), 7.52 (s, 1H), 6.86 (dd, 1H), 5.88 (d, 1H), 5.49 (d, 1H). $^{13}$C NMR ($CD_2Cl_2$, 75 MHz, ppm): 174.17, 150.76, 133.70, 128.85, 126.34, 123.83, 118.44. Anal. Calcd for $C_{12}H_6O_2S_2$: C, 58.52; H, 2.46; O, 12.99. Found: C, 58.44; H, 2.50; O, 12.86.

**2.4. Synthesis of Poly(2-vinylbenzo[1,2-b:4,5-b′]-dithiophene-4,8-dione) (4).** Monomer **3** was polymerized according the following general procedure:

50 mg of monomer **3** (0.09 mmol) and 0.00101 mmol (0.05 equiv) of initiator were dissolved in a specific amount of solvent (see Table 1). The reaction mixture was purged with dry argon for 20 min and was stirred for 16 h at a specific temperature. After the mixture cooled to room temperature, polymer **4** was purified by repeated precipitation in acetone collected by centrifugation followed by drying under vacuum. Anal. Calcd for $C_{12}H_6O_2S_2$: C, 58.52; H, 2.46; O, 12.99. Found: C, 58.62; H, 2.56; O, 12.62.

**2.5. Electrochemical Analysis.** A three electrode setup was used (WE, glassy carbon disk (diameter 2 mm); RE, $AgNO_3$/Ag in $CH_3CN$ 0.1 M *n*-$Bu_4NPF_6$; CE, Pt wire) for cyclic voltammetry. The redox couple of ferrocenium/ferrocene ($Fc^+$/Fc) was utilized as internal standard. All electrolytes were degassed with dry argon and all measurements were performed under argon atmosphere.

**2.6. Preparation of Electrodes.** Electrodes were prepared by adding a solution of PVBDT (**4**) and poly(vinylidenefluoride) (PVDF; Sigma-Aldrich) in NMP (10 mg/mL) to vapor-grown carbonfibers (VGCF; Sigma-Aldrich) as conducting additives (ratio: 1/8/1 m/m/m). These materials were mixed in a mortar for 10 min and more NMP was added to yield a paste. The thus-obtained paste was coated on graphite foil (Alfa Aesar) applying a doctor blading method. Subsequently, NMP was removed by heating the electrodes at 40 °C under high vacuum for 24 h.

**2.7. Preparation of Coin Cells.** A solution of PVBDT (**4**) and poly(vinylidenefluoride) (PVDF, Sigma-Aldrich) in NMP (10 mg/


DOI: 10.1021/am5060959
ACS Appl. Mater. Interfaces 2015, 7, 3473−3479

mL) was added to multiwalled carbon nanotubes (MWCNT, L 6−13 nm × 2.5−20 μm; Sigma-Aldrich) as a conducting additive (ratio: 1/8/1 m/m/m). More NMP was added, and the materials were mixed in a mortar for 10 min. The paste was coated on aluminum foil (thickness, 0.015 mm; MTI Corporation) applying the doctor blading method. Subsequently, the NMP was removed at 40 °C under high vacuum for 24 h. After drying, the amount of active material on the electrode was determined on the basis of the weight of the electrodes. The coin cells (type 2032) were manufactured under argon atmosphere. Suitable, round composite electrodes (15 mm diameter) were cut with a MTI Corporation Precision Disc Cutter T-0.6. The crude electrode was sandwiched between two sheets of paper. This electrode was employed as a cathode and placed into the bottom cell case and separated from the lithium anode by a porous polypropylene membrane (celgard, MTI Corporation). On top of the lithium anode (lithium foil, Sigma-Aldrich), a stainless steal space (diameter, 15.5 mm; thickness, 0.3 mm, MTI Corporation) and a stainless steal wave spring (diameter, 14.5 mm; thickness, 1.2 mm) were placed. The cell was filled with electrolyte (ethylene carbonate, dimethyl carbonate 1/1 m/v, 1 M lithium perchlorate) and the top cell case was placed onto the electrode. Finally, the cell was sealed with an electric crimper machine (MTI Corporation MSK-100D). Electrochemical measurements were performed after an equilibration time of 24 h. All experiments were carried out at room temperature. The charge/discharge capacities were determined based on the weight of PVBDT in the electrode.

## 3. RESULTS AND DISCUSSION

Polymer **4** was synthesized in a straightforward manner in five steps starting from the commercially available thiophene-3-carboxylic acid (Scheme 1), which was transformed to *N*,*N*′-diethylthiophene-3-carboxamide. The subsequent reaction with *n*-butyllithium yielded 4,8-dihydrobenzo[1,2-b:4,5-b′]-dithiophene-4,8-dione (**1**). Iodination of **1** was achieved by an iodination catalyzed by silver sulfate and 2-iodobenzo[1,2-b:4,5-b′]dithiophene-4,8-dione (**2**) was obtained in high yields (83%). It was subsequently transformed into 2-vinylbenzo[1,2-b:4,5-b′]dithiophene-4,8-dione (**3**) by a Stille-reaction. The vinyl group of monomer **3** is in conjugation with the aromatic quinone system and, therefore, **3** can be polymerized applying free radical polymerization techniques. For this purpose, suitable polymerization conditions (initiator, solvent, etc.) for **3** were evaluated. Monomer **3** is hardly soluble in common solvents used for the free radical polymerization (e.g., tetrahydrofuran and chloroform), but exhibits sufficient solubility in aprotic polar solvents such as 1,2-dichloroethane (DCE), *N*,*N*′-dimethylformamide (DMF), *N*,*N*′-dimethylacetamide (DMAc), dimethyl sulfoxide (DMSO), and/or *N*-methyl-2-pyrrolidone (NMP), in particular at elevated temperatures. The free radical polymerization was carried out utilizing 5 mol % of AIBN as initiator. This uncontrolled polymerization technique results generally in polymers with a large molar mass distribution. Polymers synthesized with DCE, DMF, DMAc, and DMSO as solvents precipitated, and low yields in the range of 8 to 25% were obtained. In NMP, the polymerization proceeded without precipitation and **4** could be obtained in 40% yield. Size-exclusion chromatograms investigations of all polymers reveal bimodal distributions, most likely caused by recombination reactions (Figure 1a), because both distributions have the same UV−vis spectrum (Figures S1−S9, Supporting Information). To increase both molar mass and yield several different initiators at appropriate reaction temperatures were investigated (Figure 1b). The best results were obtained utilizing 5 mol % *tert*-butylperoxybenzoate as initiator at a temperature of 100 °C. Finally, the amount of *tert*-butylperoxybenzoate was varied between 1 and 10 mol %, but polymers were obtained in comparable yields with similar molar masses and molar-mass distributions (Figure S10, Supporting Information). The results of the polymerizations are summarized in Table 1.

**Scheme 1. Schematic Representation of the Synthesis of Polymer 4**

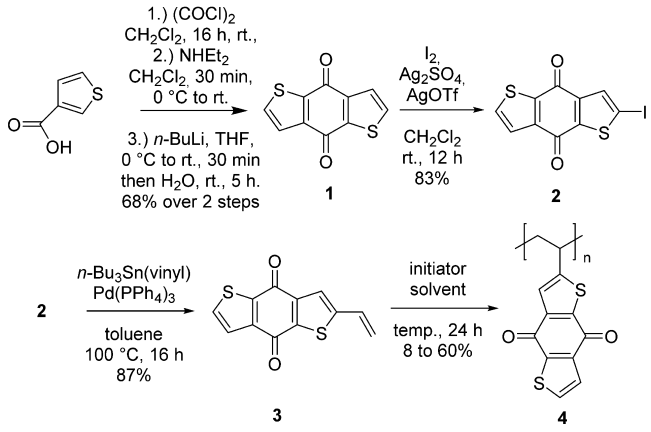


Thermal analysis revealed a high thermal stability up to around 260 °C, which is important with regard to the safety of Li-ion batteries (Figure S11, Supporting Information).

Experimental studies on the redox properties of monomer **3** were carried out using cyclic voltammetry in acetonitrile with 0.1 M tetrabutylammonium perchlorate. The monomer reveals two quasi-reversible reductions at $(E_{pa} + E_{pc})/2 = -0.97$ V and $(E_{pa} + E_{pc})/2 = -1.54$ V vs $Fc^+/Fc$, corresponding to the reductions from the quinone to the semiquinone and from the semiquione to the dianione, respectively (Figure 2). The utilization of lithium perchlorate as supporting electrolyte shifts the redox potentials to more positive values (−0.74 and −0.90 V vs $Fc^+/Fc$) and their reoxidations collapse to a single wave (−0.66 V vs $Fc^+/Fc$), most probably caused by the coordination of the oxygen atoms to the lithium atom.[30,31] In DMF with 0.1 M lithium perchlorate, the ion pairing effect of the lithium ion is weaker and, therefore, the second reduction of **3** appears at −1.39 V vs $Fc^+/Fc$ (Figure 3).[30] The electrochemical behavior of polymer **4** was examined in DMF with 0.1 M lithium perchlorate as supporting electrolyte. It exhibits two quasi-reversible reductions at −1.03 and −1.33 V vs $Fc^+/Fc$ similar to the redox behavior of monomer **3**. This finding proves that the polymer backbone has only a negligible influence on the redox behavior in solution.

The stabilities of both redox pairs were further investigated by UV−vis-NIR spectroelectrochemical studies of monomer **3** in acetonitrile. The utilization of lithium perchlorate as supporting salt leads to a merging of the reductions, thus a differentiation between the single reduction processes with UV−vis-NIR spectroscopy was not possible. During the reduction process, the intensity of the absorptions at 280 and 350 nm decrease, but are not restored completely upon reoxidation (Figure S16, Supporting Information). To obtain deeper insight of the redox process, UV−vis-NIR spectroelectrochemistry was performed with 0.1 M tetrabutylammonium perchlorate as the supporting electrolyte (Figure 4). The first reduction reveals to be a defined and stable electrochemical process. During the reduction, the strong absorption at 280 nm


DOI: 10.1021/am5060959
ACS Appl. Mater. Interfaces 2015, 7, 3473−3479

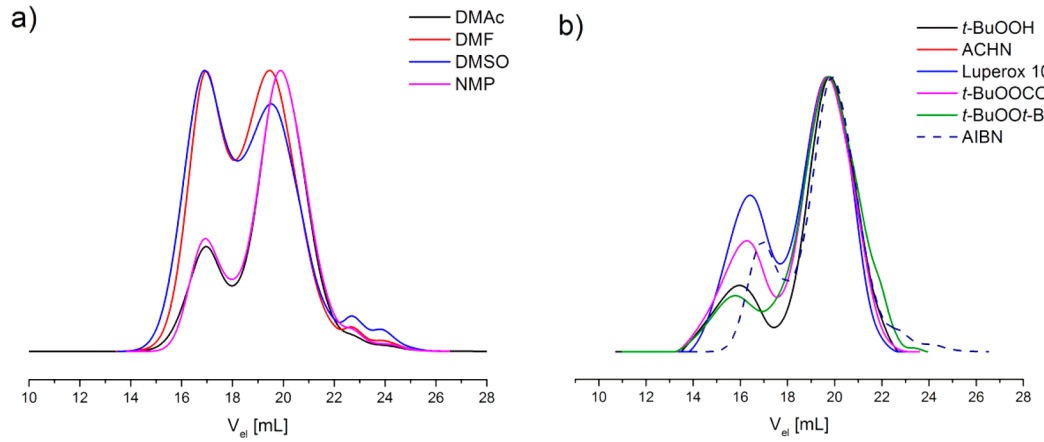


**Figure 1.** (a) Size-exclusion chromatograms of **4** synthesized with 5 mol % AIBN as initiator at 70 °C in different solvents. Eluent: DMAc, 0.21% LiCl, polystyrene standard, RI detector. (b) Size-exclusion chromatograms of **4** synthesized with 5 mol % of different initiators in NMP. Eluent: DMAc, 0.21% LiCl, polystyrene standard, RI detector.

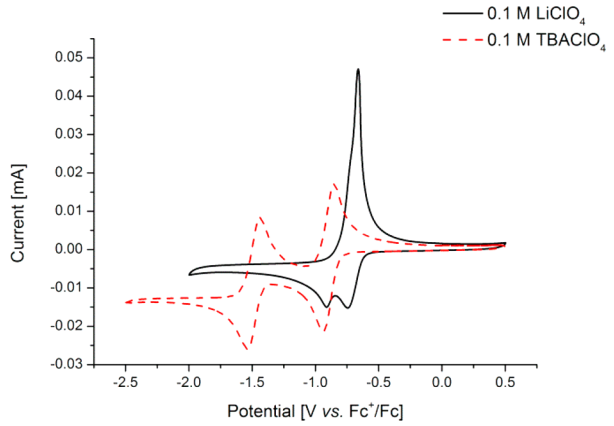


**Figure 2.** Cyclic voltammograms of monomer **3** (4 mmol/mL) in acetonitrile with 0.1 M tetrabutylammonium perchlorate (dashed red line) and lithium perchlorate (solid black line) as supporting electrolyte at a scan rate of 100 mV/s.

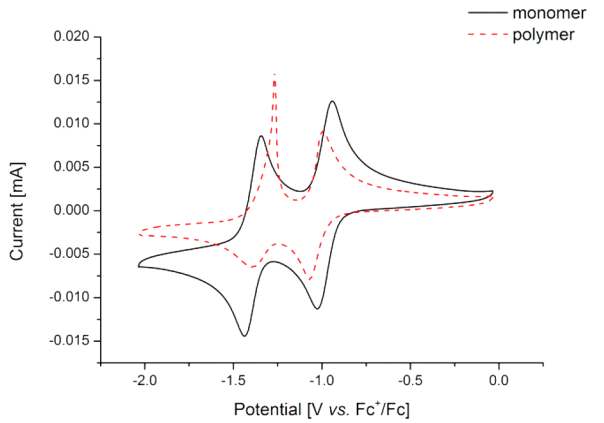


**Figure 3.** Cyclic voltammograms of monomer **3** (4 mmol/mL) (solid black line) and polymer **4** (4 mmol/mL) (dashed red line) in DMF with 0.1 M lithium perchlorate as supporting electrolyte at a scan rate of 100 mV/s.

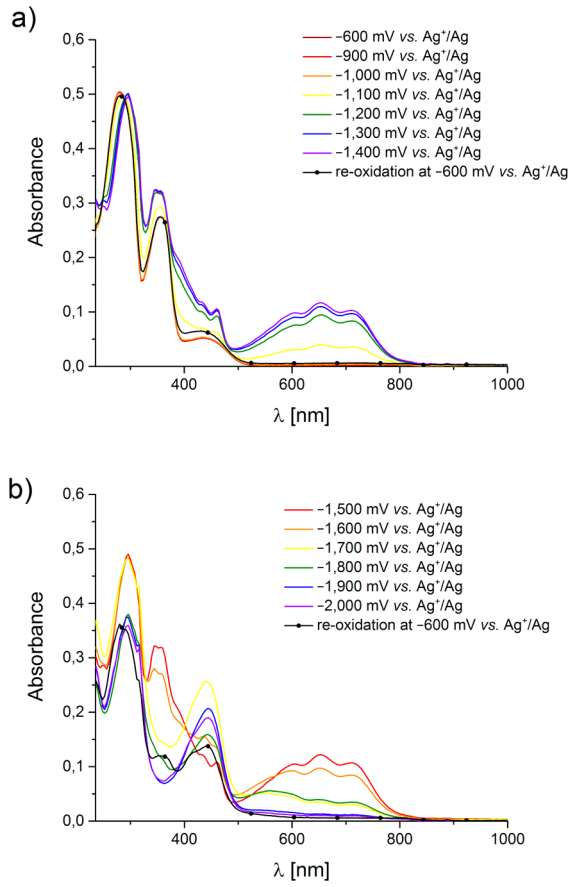


**Figure 4.** UV−vis-NIR spectroelectrochemistry of monomer **3** (acetonitrile, 0.1 M tetrabutylammonium perchlorate. RE: $AgNO_3$/Ag = 0.08 V vs $Fc^+$/Fc).

is shifted to slightly higher wavelengths accompanied by the appearance of a very broad absorption feature in the long-wavelength region. Isosbestic points emerge at 285, 370, and 480 nm, indicating the presence of only two species. The application of a reoxidizing potential restores the original spectrum nearly completely, confirming the electrochemical stability of the first redox pair. During the second reduction, the strong absorption bands at 295, 352 nm, and in the long-wavelength region decrease, accompanied by an increase of an absorption signal at around 445 nm. The spectral change of the second reduction reveals no isosbestic points. Thus, more than two species are involved in the second reduction process. A reoxidation restores the initial spectrum only partly, indicating


DOI: 10.1021/am5060959
ACS Appl. Mater. Interfaces 2015, 7, 3473−3479

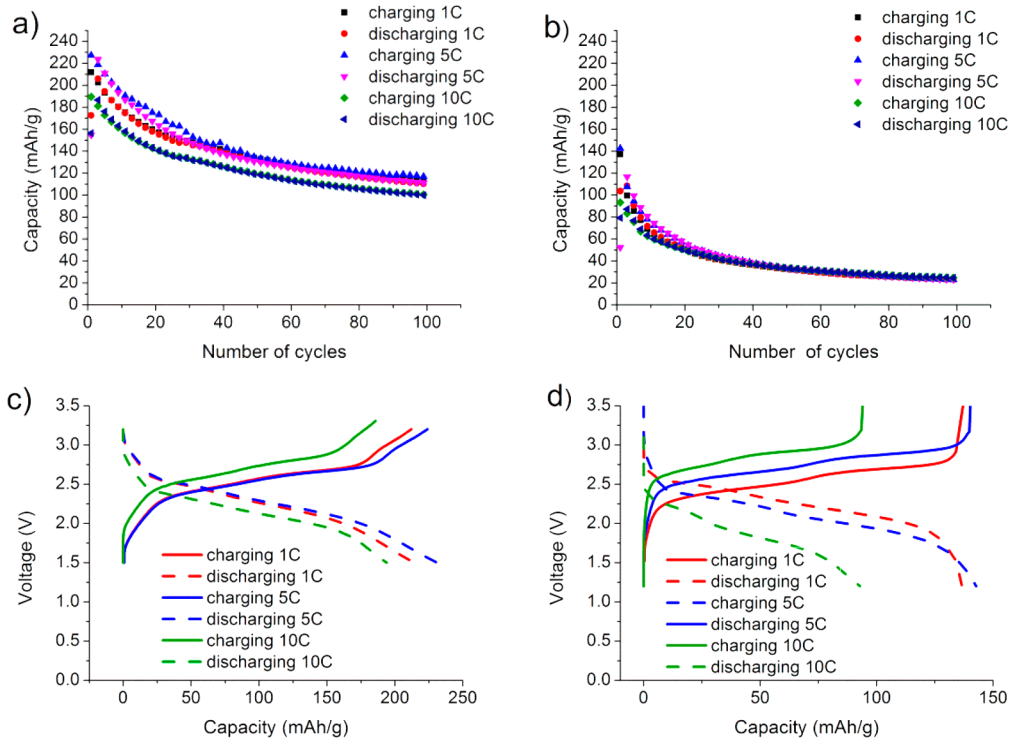


**Figure 5.** (a, b) Capacity development during extended charge/discharge cycling (100 cycles) of Li-organic batteries with composite electrodes of **4**/MWCNT/PVdF 10/80/10 and 40/50/10 m/m/m in EC/DMC 1/1 m/v, 1 M $LiClO_4$. (c, d) Charge/discharge curves (capacity vs potential) of Li-organic batteries with composite electrodes of **4**/MWCNT/PVdF 10/80/10 and 40/50/10 m/m/m in EC/DMC 1/1 m/v, 1 M $LiClO_4$ of the 2nd charge/discharge cycle at different charging speeds.

that side reaction(s) take place during the second reduction process, most probably occurring at the unsubstituted two-position of the thiophene moiety.

The solid-state electrochemical behavior of polymer **4** was investigated in a composite electrode. Vapor-grown carbon nanofibers (VGCF) were used as conductive and poly(vinylidenefluoride) as binding additive. The compounds were mixed with NMP to yield a paste and were spread onto a graphite foil. After drying the electrode under reduced pressure it was subsequently used for electrochemical measurements. Scanning electron microscopy (SEM) images of the electrodes display a porous structure and the presence of the polymer within the electrode was proven using SEM-EDX measurements (Figures S17−S19, Supporting Information).

Cyclic voltammograms of the composite electrodes containing polymer **4** (see the Supporting Information) in ethylene carbonate/dimethyl carbonate 1/1 m/v with 1 M lithium perchlorate as the supporting electrolyte, measured in a beaker-type cell, displays one broad reduction wave at −1.17 V vs $Fc^+$/Fc and one reoxidation wave at −0.73 V vs $Fc^+$/Fc (5 mV/s). The large peak split, which is reduced at lower scanrates, indicates a limited charge transfer within the electrodes (Figure S20, Supporting Information). For multiple cycles, the electrolyte remained colorless, indicating that no significant elution of the polymer takes place.

The charge/discharge behavior of both monomer and polymer was studied in lithium-organic coin-type cells equipped with a monomer/polymer composite electrode with different ratios of active material. In general, the batteries show a reversible one-stage charge/discharge behavior. All batteries exhibit a capacity drop over cycling, possibly due to side reactions, such as an electrophilic attack, dimerization, or irreversible binding of electrolyte cations. This capacity drop is more pronounced at batteries equipped with the monomer due to dissolution of the monomer into the electrolyte during charge/discharging (Figure S21, Supporting Information). In contrast, dissolution of the active polymer can be precluded as the electrolytes are nearly colorless after charge/discharge cycling. The performance of the batteries depends on both the amount of active material and the charging speed. The charging speed, however, does not influence the capacity drop, but affects slightly the coulombic efficiency and the cell potential. Coin cells with low active-material content at charge/discharge speeds of 1C exhibit a plateau at 2.59 V for charging and 2.23 V for discharging, which is in good agreement with the redox potential of the polymer in the solid state. The battery system shows high rate capability. The coin-type cells with 10 wt % active material reveal a high material activity of 87 to 100% (190 to 219 mAh/g). The slight overcapacities may derive from weighing error of the electrodes, double layer formation or small capacitive influence of the conductive additive. After 100 charge/discharge cycles, the capacity drops to 100 to 116 mAh/g, equal to a material activity of 46 to 54% (Figure 5a). The cells were charged at different rates (1C, 5C, 10C). A rate of *n*C corresponds to a full discharge in 1/*n* h. Even at 10C (corresponding to a complete discharge within 6 min), the capacity was 87% of the capacity at 1C. However, polarization of the electrodes is observed leading to plateaus at 2.76 V for charging and at 2.10 V for discharging (Figure 5c).

Similar results were obtained using electrodes containing 20 and 30 wt % of active material (Figure S22, Supporting Information). However, the material activity is at around 50%, which is further reduced upon cycling to approximately 30% after 100 cycles. Coin-type cells with 40 wt % active material


DOI: 10.1021/am5060959
*ACS Appl. Mater. Interfaces* 2015, 7, 3473−3479

follow this trend. The material activity is mostly independent from the charging speed and between 40 and 50 (Figure 5b). After 100 cycles, the capacity drops to 36 mAh/g (15% material activity). The gap between the charge/discharge plateaus is quite narrow at a charging speed of 1C (2.63 V for charging and 2.17 V for discharging) for a redox reaction involving two electrons redox, but is significantly larger at 10C (30 wt %: 3.00 V of charging and 2.06 V for discharging (Figure S21d, Supporting Information); 40 wt %: 2.90 V for charging and 1.83 V for discharging) (Figure 5d).

## 4. CONCLUSION

The redox-active monomer 2-vinylbenzo[1,2-b:4,5-b′]-dithiophene-4,8-dione (**3**) was synthesized in high yields and polymerized using the free radical polymerization technique. The polymerization was optimized to yield PVBDT in sufficiently high molar masses, which allow its application as an active material in Li-organic batteries. The electrochemical behavior of both monomer and polymer was investigated by cyclic voltammetry. Thereby, the usage of lithium salts as supporting electrolyte leads to a shift of the redox process to more positive potentials and a merging of the two reoxidation signals to one, leading to a one staged charge/discharge behavior. PVBDT was employed in a composite electrode as an active cathode material in Li-organic batteries. The influence of the charging speed and the amount of active material in the composite electrode on the performance of the battery were investigated. Electrodes with a low amount of active material (10 wt %) perform best and exhibit a capacity of 217 mAh/g (100% material activity) at an average cell voltage of 2.45 V for the first charge/discharge cycle. Upon cycling, the capacity drops, possibly because the redox reaction is not completely side reaction free and after 100 cycles the battery exhibits 114 mAh/g (52% active material). Furthermore, the battery can be charged with negligible capacity loss at a fast charging speed of 10C. Batteries with higher active material content were also investigated but showed lower capacities due to poor material activity.

## ■ ASSOCIATED CONTENT

### Supporting Information

3D SEC data of all polymers, TGA analysis, cyclic voltammograms of monomer in solution and polymer both in solution and in the solid state, UV−vis-NIR spectroelectrochemistry analysis, SEM images of the electrodes, EDX analysis of a composite electrode, and battery performances with 20 and 30 wt % active material. This material is available free of charge via the Internet at http://pubs.acs.org.

## ■ AUTHOR INFORMATION

### Corresponding Author

*U. S. Schubert. E-mail: ulrich.schubert@uni-jena.de. Tel.: +49 3641 948200. Fax: +49 3641 948202. Homepage: www.schubert-group.com.

### Notes

The authors declare no competing financial interest.

## ■ ACKNOWLEDGMENTS

The authors thank the Bundesministerium für Bildung und Forschung, the European Social Fund (ESF), the Thüringer Aufbaubank (TAB) and the Thuringian Ministry of Economy, Employment and Technology (TMWAT) for financial support.

## ■ REFERENCES

(1) Chen, H.; Armand, M.; Demailly, G.; Dolhem, F.; Poizot, P.; Tarascon, J.-M. From Biomass to a Renewable LiXC6O6 Organic Electrode for Sustainable Li-Ion Batteries. *ChemSusChem* **2008**, *1*, 348−355.

(2) Nishide, H.; Oyaizu, K. Toward Flexible Batteries. *Science* **2008**, *319*, 737−738.

(3) Jahnert, T.; Hager, M. D.; Schubert, U. S. Application of Phenolic Radicals for Antioxidants, as Active Materials in Batteries, Magnetic Materials and Ligands for Metal-Complexes. *J. Mater. Chem. A* **2014**, *2*, 15234−15251.

(4) Janoschka, T.; Hager, M. D.; Schubert, U. S. Powering up the Future: Radical Polymers for Battery Applications. *Adv. Mater.* **2012**, *24*, 6397−6409.

(5) Song, Z.; Zhou, H. Towards Sustainable and Versatile Energy Storage Devices: An Overview of Organic Electrode Materials. *Energy Environ. Sci.* **2013**, *6*, 2280−2301.

(6) Alt, H.; Binder, H.; Kohling, A.; Sandsted, G. Quinones as Rechargeable and Regenerable Battery Cathode Materials. *J. Electrochem. Soc.* **1971**, *118*, 1950−1953.

(7) Alt, H.; Binder, H.; Sandsted, G.; Kohling, A. Investigation into Use of Quinone Compounds for Battery Cathodes. *Electrochim. Acta* **1972**, *17*, 873−887.

(8) Chen, H.; Armand, M.; Courty, M.; Jiang, M.; Grey, C. P.; Dolhem, F.; Tarascon, J.-M.; Poizot, P. Lithium Salt of Tetrahydroxybenzoquinone: Toward the Development of a Sustainable Li-Ion Battery. *J. Am. Chem. Soc.* **2009**, *131*, 8984−8988.

(9) Yao, M.; Senoh, H.; Yamazaki, S.-i.; Siroma, Z.; Sakai, T.; Yasuda, K. High-Capacity Organic Positive-Electrode Material Based on a Benzoquinone Derivative for Use in Rechargeable Lithium Batteries. *J. Power Sources* **2010**, *195*, 8336−8340.

(10) Shimizu, A.; Tsujii, Y.; Kuramoto, H.; Nokami, T.; Inatomi, Y.; Hojo, N.; Yoshida, J.-i. Nitrogen-Containing Polycyclic Quinones as Cathode Materials for Lithium-Ion Batteries with Increased Voltage. *Energy Technol.* **2014**, *2*, 155−158.

(11) Zeng, R.-h.; Li, X.-p.; Qiu, Y.-c.; Li, W.-s.; Yi, J.; Lu, D.-s.; Tan, C.-l.; Xu, M.-q. Synthesis and Properties of a Lithium-Organic Coordination Compound as Lithium-Inserted Material for Lithium Ion Batteries. *Electrochem. Commun.* **2010**, *12*, 1253−1256.

(12) Chen, H.; Poizot, P.; Dolhem, F.; Basir, N. I.; Mentré, O.; Tarascon, J.-M. Electrochemical Reactivity of Lithium Chloranilate vs Li and Crystal Structures of the Hydrated Phases. *Electrochem. Solid-State Lett.* **2009**, *12*, A102−A106.

(13) Liang, Y.; Zhang, P.; Chen, J. Function-Oriented Design of Conjugated Carbonyl Compound Electrodes for High Energy Lithium Batteries. *Chem. Sci.* **2013**, *4*, 1330−1337.

(14) Iordache, A.; Maurel, V.; Mouesca, J.-M.; Pécaut, J.; Dubois, L.; Gutel, T. Monothioanthraquinone as an Organic Active Material for Greener Lithium Batteries. *J. Power Sources* **2014**, *267*, 553−559.

(15) Liang, Y.; Zhang, P.; Yang, S.; Tao, Z.; Chen, J. Fused Heteroaromatic Organic Compounds for High-Power Electrodes of Rechargeable Lithium Batteries. *Adv. Energy Mater.* **2013**, *3*, 600−605.

(16) Shimizu, A.; Kuramoto, H.; Tsujii, Y.; Nokami, T.; Inatomi, Y.; Hojo, N.; Suzuki, H.; Yoshida, J.-i. Introduction of Two Lithiooxycarbonyl Groups Enhances Cyclability of Lithium Batteries with Organic Cathode Materials. *J. Power Sources* **2014**, *260*, 211−217.

(17) Wan, W.; Lee, H.; Yu, X.; Wang, C.; Nam, K.-W.; Yang, X.-Q.; Zhou, H. Tuning the Electrochemical Performances of Anthraquinone Organic Cathode Materials for Li-Ion Batteries through the Sulfonic Sodium Functional Group. *RSC Adv.* **2014**, *4*, 19878−19882.

(18) Gottis, S.; Barrès, A.-L.; Dolhem, F.; Poizot, P. Voltage Gain in Lithiated Enolate-based Organic Cathode Materials by Isomeric Effect. *ACS Appl. Mater. Interfaces* **2014**, *6*, 10870−10876.

(19) Hanyu, Y.; Ganbe, Y.; Honma, I. Application of Quinonic Cathode Compounds for Quasi-solid Lithium Batteries. *J. Power Sources* **2013**, *221*, 186−190.

(20) Häringer, D.; Novák, P.; Haas, O.; Piro, B.; Pham, M. C. Poly(5-amino-1,4-naphthoquinone), a Novel Lithium-Inserting Electroactive



DOI: 10.1021/am5060959
*ACS Appl. Mater. Interfaces* 2015, 7, 3473−3479

Polymer with High Specific Charge. *J. Electrochem. Soc.* **1999**, *146*, 2393−2396.
(21) Song, Z.; Zhan, H.; Zhou, Y. Anthraquinone Based Polymer as High Performance Cathode Material for Rechargeable Lithium Batteries. *Chem. Commun.* **2009**, 448−450.
(22) Liu, K.; Zheng, J.; Zhong, G.; Yang, Y. Poly(2,5-dihydroxy-1,4-benzoquinonyl sulfide) (PDBS) as a Cathode Material for Lithium Ion Batteries. *J. Mater. Chem.* **2011**, *21*, 4125−4131.
(23) Le Gall, T.; Reiman, K. H.; Grossel, M. C.; Owen, J. R. Poly(2,5-dihydroxy-1,4-benzoquinone-3,6-methylene): A New Organic Polymer as Positive Electrode Material for Rechargeable Lithium Batteries. *J. Power Sources* **2003**, *119−121*, 316−320.
(24) Oyama, N.; Sarukawa, T.; Mochizuki, Y.; Shimomura, T.; Yamaguchi, S. Significant Effects of Poly(3,4-ethylenedioxythiophene) Additive on Redox Responses of Poly(2,5-dihydroxy-1,4-benzoquinone-3,6-methylene) Cathode for Rechargeable Li Batteries. *J. Power Sources* **2009**, *189*, 230−239.
(25) Xu, W.; Read, A.; Koech, P. K.; Hu, D.; Wang, C.; Xiao, J.; Padmaperuma, A. B.; Graff, G. L.; Liu, J.; Zhang, J.-G. Factors Affecting the Battery Performance of Anthraquinone-based Organic Cathode Materials. *J. Mater. Chem.* **2012**, *22*, 4032−4039.
(26) Oyaizu, K.; Choi, W.; Nishide, H. Functionalization of Poly(4-chloromethylstyrene) with Anthraquinone Pendants for Organic Anode-Active Materials. *Polym. Adv. Technol.* **2011**, *22*, 1242−1247.
(27) Nokami, T.; Matsuo, T.; Inatomi, Y.; Hojo, N.; Tsukagoshi, T.; Yoshizawa, H.; Shimizu, A.; Kuramoto, H.; Komae, K.; Tsuyama, H.; Yoshida, J.-i. Polymer-Bound Pyrene-4,5,9,10-tetraone for Fast-Charge and -Discharge Lithium-Ion Batteries with High Capacity. *J. Am. Chem. Soc.* **2012**, *134*, 19694−19700.
(28) Choi, W.; Harada, D.; Oyaizu, K.; Nishide, H. Aqueous Electrochemistry of Poly(vinylanthraquinone) for Anode-Active Materials in High-Density and Rechargeable Polymer/Air Batteries. *J. Am. Chem. Soc.* **2011**, *133*, 19839−19843.
(29) Hou, J.; Park, M.-H.; Zhang, S.; Yao, Y.; Chen, L.-M.; Li, J.-H.; Yang, Y. Bandgap and Molecular Energy Level Control of Conjugated Polymer Photovoltaic Materials Based on Benzo[1,2-b:4,5-b′]-dithiophene. *Macromolecules* **2008**, *41*, 6012−6018.
(30) Pletcher, D.; Thompson, H.; Microelectrode, A. Study of the Influence of Electrolyte on the Reduction of Quinones in Aprotic Solvents. *J. Chem. Soc., Faraday Trans.* **1998**, *94*, 3445−3450.
(31) Wain, A. J.; Wildgoose, G. G.; Heald, C. G. R.; Jiang, L.; Jones, T. G. J.; Compton, R. G. Electrochemical ESR and Voltammetric Studies of Lithium Ion Pairing with Electrogenerated 9,10-Anthraquinone Radical Anions Either Free in Acetonitrile Solution or Covalently Bound to Multiwalled Carbon Nanotubes. *J. Phys. Chem. B* **2005**, *109*, 3971−3978.


DOI: 10.1021/am5060959
*ACS Appl. Mater. Interfaces* 2015, 7, 3473−3479